J. Austral. Math. Soc. **21** (Series B) (1979), 65–74

ON THE UNSTEADY SQUEEZING OF A VISCOUS FLUID FROM A TUBE

F. M. SKALAK and C. Y. WANG

(Received 1 May 1978)

(Revised 24 November 1978)

Abstract

Viscous fluid is squeezed out from a shrinking (or expanding) tube whose radius varies with time as $(1-\beta t)^{\frac{1}{2}}$. The full Navier–Stokes equations reduce to a non-linear ordinary differential equation governed by a non-dimensional parameter S representing the relative importance of unsteadiness to viscosity. This paper studies the analytic solutions for large $|S|$ through the method of matched asymptotic expansions. A simple numerical scheme for integration is presented. It is found that boundary layers exist near the walls for large $|S|$. In addition, flow reversals and oscillations of the velocity profile occur for large negative S (fast expansion of the tube).

1. Introduction

The full Navier–Stokes equations including all the unsteady, viscous and inertial terms represent a set of non-linear partial differential equations with very few exact solutions. Excluding unsteady parallel and unsteady concentric cylindrical flows, where the non-linear terms vanish individually, only the following two types of exact solutions exist.

(I) Wang [5] studied a class of solutions where the non-linear terms are not zero individually but the non-linearities cancel each other. These flows include Taylor's [3] solution of vortex decay, and other impinging flows. The solutions of this type admit no rigid boundaries and the velocities vary exponentially with time.

(II) Birkhoff [2], in his study of transformation groups, noted the Navier–Stokes equations would reduce to a single non-linear ordinary differential equation if the lateral velocities are proportional to $t^{-\frac{1}{2}}$. Birkhoff's idea of similarity solutions was extended by Yang [7] to unsteady stagnation point flow and by Wang [6]

https://doi.org/10.1017/S0334270000001922 Published online by Cambridge University Press

to the squeezing of two plates. Recently Uchida and Aoki [4] also applied this transformation to the squeezing of a viscous fluid out of a shrinking cylinder. This situation occurs, for example, in physiology, when regional blood volume is reduced by the active "vasoconstriction" of the blood vessels (for example, Berne and Levy [1]).

However, Uchida and Aoki [4] only studied the shrinking tube solutions for low squeeze numbers ($|S| \leqslant 5$). This is adequate for vasoconstriction but is inadequate for the ejection of the heart ($|S| \approx 50$). The recent paper studies the behaviour of the fluid for large $|S|$ (fast squeezing and expansion). The results are important in the fluid dynamics of ventricular pumping.

2. Formulation

Let the inside tube radius be prescribed by $a(t)$. The Navier–Stokes equations then admit similarity solutions if

$$a(t) = a_0\sqrt{(1-\beta t)}, \tag{1}$$

where a_0 and β are constants. When β is positive the tube is squeezed until total collapse at $t = 1/\beta$ and when β is negative the tube is expanded indefinitely.

Let u, v be the velocities in cylindrical polar coordinates in the directions of z, r respectively. The following transformation is used

$$\eta = \frac{r^2}{a_0^2(1-\beta t)}, \tag{2}$$

$$v = \frac{-a_0\beta f(\eta)}{2\sqrt{(1-\beta t)}\sqrt{\eta}}, \tag{3}$$

$$u = \frac{\beta z f'(\eta)}{1-\beta t}, \tag{4}$$

$$p = \frac{\rho a_0^2\beta^2}{4(1-\beta t)}\left(f - \frac{f^2}{2\eta} - \frac{4\nu f'}{\beta a_0^2}\right) + \frac{2\mu\beta z^2 A}{a_0^2(1-\beta t)^2} + P(t), \tag{5}$$

where η is the normalized radius, p is the pressure, ρ is the density and ν is the kinematic viscosity of the fluid. The constant A and the function $P(t)$ are to be determined from the boundary conditions. Note that our radial variable, η, is the square of that defined by [4]. We shall consider the time interval $t < \beta^{-1}$ when $\beta > 0$ and $t > -|\beta|^{-1}$ when $\beta < 0$.

The boundary conditions are on

$$r = a(t), \quad v = da/dt, \quad u = 0, \tag{6}$$

https://doi.org/10.1017/S0334270000001922 Published online by Cambridge University Press

$$r = 0, \quad v = 0, \quad \partial u/\partial r = 0. \tag{7}$$

Using equations (2–7) the Navier–Stokes equations then reduce to an ordinary differential equation

$$\eta f'''' + 2f''' - S(\eta f''' + 2f'' + f'f'' - ff''') = 0, \tag{8}$$

with the boundary conditions

$$\lim_{\eta \to 0} \left(\frac{f}{\sqrt{\eta}} \right) = 0 \quad \text{or} \quad f(0) = 0, \tag{9}$$

$$\lim_{\eta \to 0} (\sqrt{(\eta)}\, f'') = 0, \tag{10}$$

$$f'(1) = 0, \tag{11}$$

$$f(1) = 1. \tag{12}$$

Here S is a "squeeze number" defined by

$$S \equiv \beta a_0^2/4\nu. \tag{13}$$

The character of the solutions depends heavily on the parameter S. We believe that our equation (8) is much simpler than Uchida and Aoki's equation (24). In addition, the derivatives of our function f are bounded everywhere, while the derivatives of their F are singular at the origin. Equation (8) can be converted to the equation (24) of reference [4] by the following substitution: $f \to -F/\alpha$, $\eta \to \eta^2$, $S \to -\alpha/2$, $A \to -K/8\alpha$, $\beta \to -2\alpha\nu/a_0^2$.

3. Asymptotic solution for large, positive S

This is the case for fast transient squeezing. We set $\varepsilon^2 \equiv 1/S \ll 1$ and use the method of matched asymptotic expansions. In the interior let

$$f = F_0 + \varepsilon F_1 + \ldots. \tag{14}$$

We substitute (14) into (8). The leading terms are

$$\eta F_0''' + 2F_0'' + F_0' F_0'' - F_0 F_0''' = 0, \tag{15}$$

with the boundary conditions

$$F_0(0) = 0, \quad F_0(1) = 1, \quad \lim_{\eta \to 0} \sqrt{(\eta)}\, F_0''(\eta) = 0. \tag{16}$$

The solution is the potential flow

$$F_0 = \eta. \tag{17}$$

https://doi.org/10.1017/S0334270000001922 Published online by Cambridge University Press

Since the boundary layer is on $\eta = 1$, we define a stretched variable

$$\zeta = (1-\eta)/\varepsilon, \tag{18}$$

$$f = 1 - \varepsilon g_1(\zeta) - \varepsilon^2 g_2(\zeta) - \ldots, \tag{19}$$

$$A = (1/\varepsilon^2)(A_0 + \varepsilon A_1 + \ldots). \tag{20}$$

Using the transformations (18–20), the leading terms of equation (8) are

$$g_1''' - \zeta g_1''' - 2g_1'' - g_1' g_1'' + g_1 g_1''' = 0 \tag{21}$$

or after integration

$$g_1''' - \zeta g_1'' - g_1' - g_1' g_1' + g_1 g_1'' = A_0. \tag{22}$$

The matching boundary conditions are

$$g_1 \sim \zeta \quad \text{as} \quad \zeta \to \infty, \qquad g_1(0) = 0, \quad g_1'(0) = 0. \tag{23}$$

We are fortunate that the boundary layer equations (22, 23) admit an exact solution

$$g_1 = \zeta - (1/\sqrt{2}) + (1/\sqrt{2})\, e^{-\sqrt{(2)}\zeta}, \tag{24}$$

$$A_0 = -2.$$

The first-order interior solution F_1 is also found to satisfy equation (15). Matching with the boundary layer, we find

$$F_1 = (1/\sqrt{2})\,\eta. \tag{25}$$

Again from equations (8, 18, 19) the second-order boundary layer equation is

$$g_2''' - \zeta g_1''' - g_1'' - [\zeta g_2'' + g_2' + 2g_1' g_2' - g_1 g_2'' - g_2 g_1''] = A_1. \tag{26}$$

Using equations (8) and (19) the matching boundary conditions are

$$g_2(0) = g_2'(0) = 0, \tag{27}$$

$$g_2(\infty) \sim (1/\sqrt{2})\,\zeta. \tag{28}$$

From equations (26) and (28) we find

$$A_1 = -3/\sqrt{2}. \tag{29}$$

https://doi.org/10.1017/S0334270000001922 Published online by Cambridge University Press

Without solving for g_2, it follows that

$$g_2'''(0) = -1/\sqrt{2}. \tag{30}$$

The composite solution is then

$$f = \eta + (\varepsilon/\sqrt{2})\,\eta - (\varepsilon/\sqrt{2})\,e^{-\sqrt{(2)}\xi} + O(\varepsilon^2), \tag{31}$$

$$A = (-2/\varepsilon^2) - (3/\sqrt{(2)}\,\varepsilon) + O(1) = f''(1) + f'''(1), \tag{32}$$

$$f''(1) = (-\sqrt{2}/\varepsilon) + O(1), \tag{33}$$

$$f'''(1) = (-2/\varepsilon^2) - (1/\sqrt{(2)}\,\varepsilon) + O(1). \tag{34}$$

4. Asymptotic solution for large, negative S

Large negative S means fast transient expansion of the tube with a subsequent suction of fluid from the ends. Since vorticity is transported from the ends the interior is sensitive to the entrance conditions. It is not certain whether the solutions are unique.

Assuming a boundary layer on $\eta = 1$, we set $\delta^2 = |S|^{-1}$ and obtain an interior solution similar to equation (17). The stretching

$$\xi = (1-\eta)/\delta, \tag{35}$$

$$f = 1 - \delta h_1(\xi) - \delta^2 h_2(\xi) - \ldots, \tag{36}$$

yields

$$h_1'''' + \xi h_1''' + 2h_1'' + h_1' h_1'' - h_1 h_1''' = 0, \tag{37}$$

$$h_1(\infty) \to \xi, \quad h_1(0) = h_1'(0) = 0. \tag{38}$$

The conditions for exponential decay of the boundary layer can be obtained by setting

$$h_1 = \xi + c_1 + \phi(\xi), \tag{39}$$

where c_1 is a constant and ϕ is small. Equation (37) is then linearized to give

$$\phi'''' - c_1 \phi''' + 3\phi'' = 0. \tag{40}$$

This yields

$$\phi \sim \exp\{\tfrac{1}{2}[c_1 \pm \sqrt{(c_1^2 - 12)}]\,\xi\}. \tag{41}$$

Exponential decay is possible when $c_1 < 0$. Further, the solution is oscillatory (in ξ) when $|c_1| < 2\sqrt{3}$.

https://doi.org/10.1017/S0334270000001922 Published online by Cambridge University Press

Numerical solutions of equations (37–38) by the shooting method do not appear to be unique. One solution (Fig. 1) yields $h_1''(0) = -1.831249$, $h_1'''(0) = 2$ and $c_1 = -3.38$. Although $|c_1| < 2\sqrt{3}$ here, the oscillations for large ξ are not apparent in the figure due to the long period [approximately 16.4 from equation (41)] and the fast decay. Other solutions yield results similar to Fig. 1.

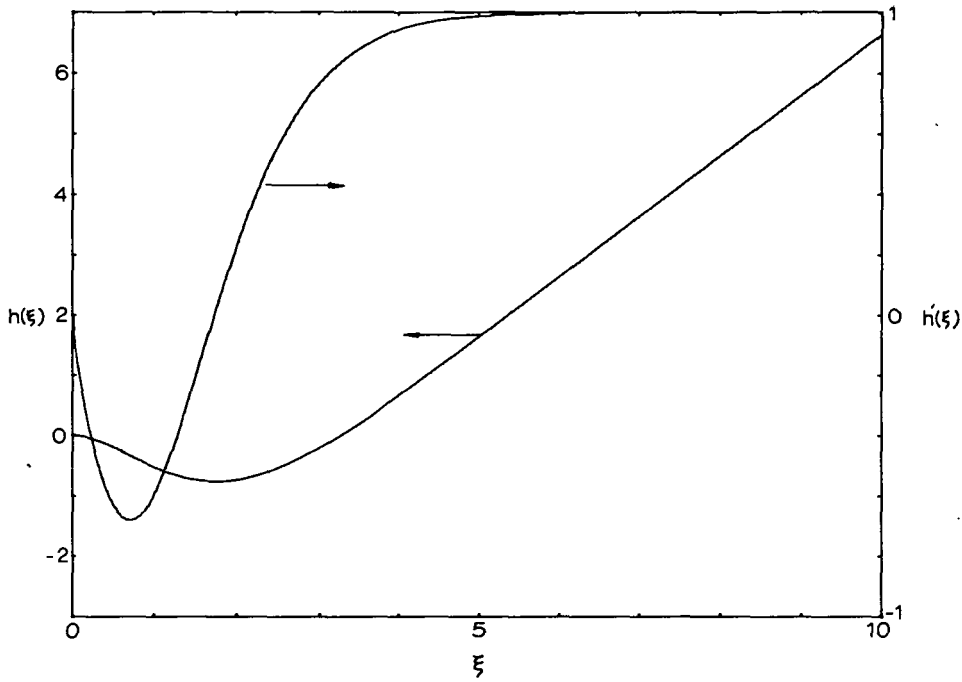

Fig. 1. Numerical solution of the boundary layer equations (37–38).

We note the boundary layers for large negative S have inflection points for small ξ. In contrast, the boundary layer for large positive S, equation (24), is monotonic.

A similar uniformly valid solution can be constructed

$$f = \eta - \delta c_1 \eta - \delta[h_1(\xi) - \xi - c_1] + O(\delta^2). \tag{42}$$

5. Numerical solution

Equations (8–12) may be integrated numerically to yield exact solutions for any S. Uchida and Aoki [4] used a two-parameter shooting scheme. However, this

https://doi.org/10.1017/S0334270000001922 Published online by Cambridge University Press

difficult two-point boundary value problem can be much simplified by transforming the dependent and independent variables as follows [6]:

$$f(\eta) = G(\lambda)/|S|, \tag{43}$$

$$\lambda = |S|\eta. \tag{44}$$

Equation (8) then yields

$$\lambda G''' + 2G''' - (\operatorname{sign} S)(\lambda G''' + 2G'' + G'G'' - GG''') = 0, \tag{45}$$

$$G(0) = 0, \quad \lim_{\lambda \to 0} \sqrt{(\lambda)}\, G''(\lambda) = 0, \tag{46}$$

$$G(|S|) = |S|, \quad G'(|S|) = 0. \tag{47}$$

Since equation (45) is singular at $\lambda = 0$, an analytic expansion is needed to *start* the numerical integration. The following method is used. For $0 \leqslant \lambda \leqslant \lambda_T$ we guess $G'(0)$ and $G''(0)$ and obtain all higher derivatives from equation (45). A Taylor series is then constructed

$$G(\lambda) \approx \sum_{n=0}^{N} \frac{\lambda^n}{n!} \frac{d^n G}{d\lambda^n}\bigg|_0. \tag{48}$$

For a given $N \geqslant 2$, the maximum range for Taylor series approximation λ_T is determined by requiring

$$(\lambda^n/n!)\, G^{(N+1)}(0) \leqslant 10^{-10}, \quad n = N+1, N, N-1, N-2. \tag{49}$$

Then using equation (48) we calculate $G(\lambda_T)$, $G'(\lambda_T)$, $G''(\lambda_T)$, $G'''(\lambda_T)$ from which equation (45) is integrated as an initial value problem for $\lambda \geqslant \lambda_T$ by the fourth-order Runge–Kutta algorithm until $G'(\lambda^*) = 0$. A solution is obtained if the value of $G(\lambda^*) - \lambda^*$ is zero. If not we can adjust *either* $G'(0)$ *or* $G''(0)$ and try again. The problem is thus reduced to a much simpler one-parameter shooting algorithm. The disadvantage is that S shall be determined *a posteriori*.

After a solution is found S is then obtained by

$$S = (\operatorname{sign} S)\, \lambda^*. \tag{50}$$

Our numerical results agree favorably with those published by Uchida and Aoki [4] for low S ($-0.835 \leqslant S \leqslant 5.0$). However, we are able to obtain solutions for much larger absolute values of S ($-57.78 \leqslant S \leqslant 46.0$).

Figures 2 and 3 show the axial velocity profiles $f'(\eta)$ plotted against $\sqrt{\eta}$ ($\eta^{\frac{1}{2}}$ is proportional to the radius r). For large positive S (fast squeeze) we see the velocity profile is similar to those published by Uchida and Aoki [4] except the boundary layer character is more obvious. For large negative S (fast expansion) the results are quite different. As S becomes more negative the region of reverse flow increases and then decreases. In the meantime, oscillations of the velocity profile appear and become more pronounced.

https://doi.org/10.1017/S0334270000001922 Published online by Cambridge University Press

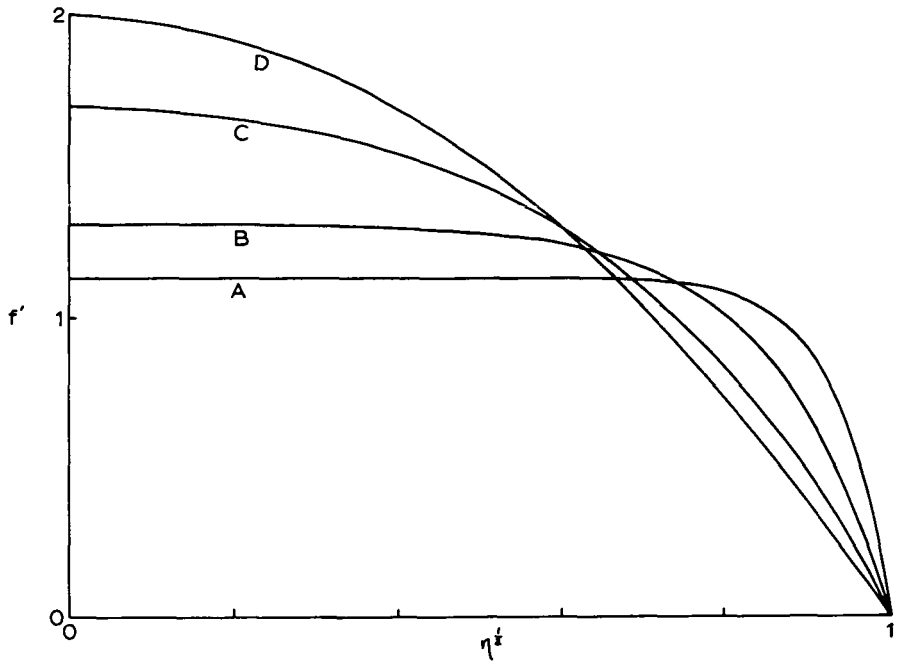

Fig. 2. Axial velocity profiles for squeezing: $A : S = 30.416$; $B : S = 6.145$; $C : S = 0.86085$; $D : S = 0$.

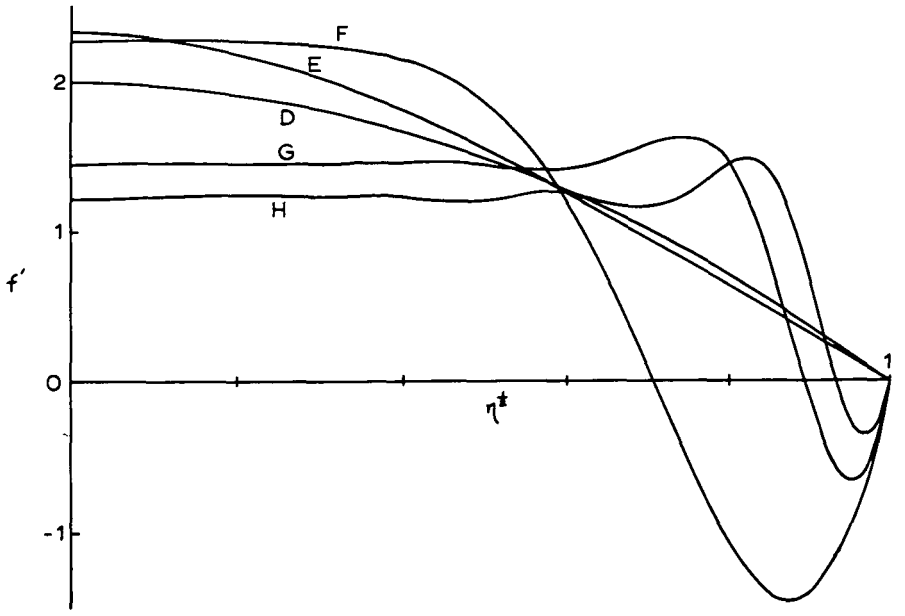

Fig. 3. Axial velocity profiles for expansion: $D : S = 0$; $E : S = -0.40737$; $F : S = -6.22206$; $G : S = -33.683$; $H : S = -57.780$.

https://doi.org/10.1017/S0334270000001922 Published online by Cambridge University Press

6. Discussion

Table 1 shows a comparison of the results from three different methods. It is seen that the series expansion obtained by Uchida and Aoki [4] compares well with exact numerical integration for small $|S|$ while our matched asymptotic expansions is adequate for large positive S.

TABLE 1

Comparison of results obtained by the various methods

	$f''(1)$		$f'''(1)$	
S	Exact numerical	Asymptotic equation (33)	Exact numerical	Asymptotic equation (34)
46.00	−10.72	−9.59	−96.55	−96.80
30.416	−8.942	−7.799	−64.507	−64.730
22.720	−7.891	−6.741	−48.658	−48.810
10.609	−5.779	−4.606	−23.289	−23.520
6.145	−4.702		−13.808	
0.86085	−2.66595		−2.13653	
		Series, [4]		Series, [4]
0.29145	−2.26218	−2.25621	−0.75261	−0.74699
0.16611	−2.15587	−2.15466	−0.43428	−0.43314
0	−2.00000	−2.00000	0.00000	0.00000
−0.11487	−1.87916	−1.87966	0.31149	0.31100
−0.40737	−1.49255	−1.52379	1.17596	1.14532
−0.73305	−0.67362		2.52706	
−6.22206	11.7685		34.9025	
−33.683	13.042		108.148	
−57.780	11.304		149.540	

We have demonstrated the possible existence of a boundary layer for large negative S which may be asymptotically oscillatory. This may also be true in the related case of the separation of two plates and has not been pointed out previously [6]. Using the same notation as in equations (35, 36, 39) one finds, in the two-plate case,

$$\phi'''' - c_1 \phi''' + (3+m)\phi'' = 0, \tag{51}$$

or

$$\phi \sim \exp\{\tfrac{1}{2}[c_1 \pm \sqrt{[c_1^2 - 4(3+m)]}\,\xi\}, \tag{52}$$

where $m = 0, 1$ represents axisymmetric and two-dimensional plates respectively. This shows exponential decay is possible if $c_1 < 0$ and the solution is oscillatory if $|c_1| < 2\sqrt{(3+m)}$.

https://doi.org/10.1017/S0334270000001922 Published online by Cambridge University Press

For $S<0$, both the separation of two plates and the expansion of a tube show marked non-uniqueness. The flow reversal and interior oscillations are characteristic for both problems. These phenomena do not occur for the small S cases studied by Uchida and Aoki [4].

REFERENCES

[1] R. M. Berne and M. N. Levy, *Cardiovascular physiology* (Mosby Co., St Louis, 1972).
[2] G. Birkhoff, *Hydrodynamics: a study in logic, fact, similitude* (Princeton University Press, 1950).
[3] G. I. Taylor, "On the decay of vortices in a viscous fluid", *Philosophical Mag.* 46 (1923), 671–674.
[4] S. Uchida and H. Aoki, "Unsteady flows in a semi-infinite contracting or expanding pipe", *J. Fluid Mech.* 82 (1977), 371–387.
[5] C.-Y. Wang, "On a class of exact solutions of the Navier–Stokes equations", *J. Appl. Mech.* 33 (1966), 696–698.
[6] C.-Y. Wang, "The squeezing of a fluid between two plates", *J. Appl. Mech.* 43 (1976), 579–583.
[7] K. T. Yang, "Unsteady laminar boundary layers in an incompressible stagnation flow", *J. Appl. Mech.* 25 (1958), 421–427.

Nuclear Eng. Division
Babcock and Wilcox Co.
Barberton, Ohio, USA
and
Departments of Mathematics and Physiology
Michigan State University
East Lansing, MI, USA

https://doi.org/10.1017/S0334270000001922 Published online by Cambridge University Press